Measurement of the Kinetic Energy and Lattice Constant in hcp Solid Helium at Temperatures 0.07–0.4 K

M. A. Adams, J. Mayers, O. Kirichek, and R. B. E. Down

ISIS Facility, Rutherford Appleton Laboratory, Chilton, OX11 0QX, United Kingdom

(Received 22 September 2006; published 22 February 2007)

The single atom kinetic energy $\boldsymbol{\kappa}$ of high purity solid hcp ^{4}He has been measured by neutron Compton scattering, at temperatures between 0.07 and 0.4 K and a pressure of 40 bar. Within statistical error of $\sim$2% no change in $\boldsymbol{\kappa}$ was observed. The values of $\boldsymbol{\kappa}$ at $\sim$0.07 K were the same in a single crystal and a polycrystalline sample and were also unaffected (within statistical error) by the addition of 10 ppm of ^{3}He. The lattice constant was also found to be independent of temperature to within 1 part in 2000. These results suggest that the supersolid transition in ^{4}He has a different microscopic origin to the superfluid transition in the liquid.

DOI: 10.1103/PhysRevLett.98.085301 PACS numbers: 67.40.−w, 03.75.Kk

The observation [1–3] of a nonclassical rotational inertia fraction (NCRIF) in solid helium at temperatures below 0.2 K has created much interest as a possible manifestation of “supersolidity”. These observations have been confirmed by a number of independent groups [4–6] although their theoretical explanation is still uncertain. The possibility of flow without viscosity in solid helium was theoretically predicted more than 30 years ago [7–9]. The latter predictions rely upon the occurrence of Bose Einstein condensation (BEC) in the solid. However, it has been shown by path integral Monte Carlo simulations [10] that in a defect free crystal of hcp helium BEC does not occur at temperatures down to 0.2 K. Measurements of the heat capacity [11] also show no anomaly, again suggesting that BEC is unlikely to be associated with the observation of the NCRIF.

Other proposed explanations are the occurrence of an incommensurate ground state with a low density of strongly correlated vacancies [12,13]. However, calculations indicate [14] that an incommensurate solid does not exist in equilibrium, although nonequilibrium vacancies relaxing on defects of polycrystalline samples could provide an explanation for the experimental observations. It has also been pointed out [15] that finite size effects imply that calculations cannot determine with any certainty whether or not hcp helium is incommensurate in the ground state. Recent measurements [16] of the melting curve at $0.01 < T < 0.5$ K also show no anomaly, suggesting that there are no significant changes in zero point vacancy concentrations in the region of the supersolid transition.

It has also been suggested [17] that the observations are due to mass flow at grain boundaries in polycrystalline samples. However, the latter experiments were performed at temperatures and pressures where liquids and solids coexist rather than under the conditions employed by Chan where (at least according to the phase diagram) only solid helium is present. Measurements of pressure driven flow have also given a null result in hcp ^{4}He [18,19].

The main motivation of the measurements described here was to provide a direct experimental test as to whether BEC plays a role in the supersolid transition. It should be noted that although the measured supersolid fraction is rather low ($\sim$1%–2%), this says nothing about the size of the condensate fraction f and any consequent change in the average kinetic energies $\boldsymbol{\kappa}$ of atoms. As Leggett [9] emphasizes, the low value of ρ_S in the solid is a result of its lack of translational symmetry. In a fluid, Leggett’s argument would imply a 100% superfluid fraction. In liquid helium the development of a $\sim$7% condensate fraction of atoms with zero kinetic energy leads to an easily measurable change in $\boldsymbol{\kappa}$ as the liquid is cooled through the superfluid transition [20,21]. There is also a $\sim$1% anomalous decrease in liquid density upon cooling from 2.17 to $\sim$1 K [22]. A secondary aim of the measurement was to determine whether there is any evidence for such an effect in the supersolid.

The measurements were performed on the VESUVIO spectrometer at the ISIS neutron source. VESUVIO uses eV neutrons to measure atomic kinetic energies and momentum distributions. The instrument detects only scattered neutrons with energies $4.908 \pm \sim 0.15$ eV. Time-of-flight measurement is then used to determine the incident neutron energy and hence the momentum and energy transfer in the scattering process. More details of the spectrometer and the data analysis procedures are given in Ref. [23].

Measurements of atomic kinetic energies by neutron scattering are possible because at very high incident neutron energies the impulse approximation (IA) [24] is valid. In the IA neutrons scatter from single atoms with conservation of kinetic energy and momentum of the neutron + nucleus. This implies that the energy transfer $\hbar\omega$ is given by

$$\hbar\,\omega = \frac{(\mathbf{p} + \hbar\mathbf{q})^2}{2M} - \frac{p^2}{2M}, \tag{1}$$

where q is the wave vector transfer in the measurement, $\mathbf{p}$

is the momentum of the struck atom before the collision, and M is the atomic mass. Rearranging this equation gives

$$y = \mathbf{p}\cdot\hat{\mathbf{q}} = \frac{M}{q}\left(\omega - \frac{\hbar q^2}{2M}\right). \tag{2}$$

Thus, by measuring ω and q, the component of the atomic momentum along the unit vector $\hat{\mathbf{q}}$ (conventionally denoted as y) can be determined for each individual scattering event. By measuring a very large number of such events, the distribution of y values $J(y)$ can be determined. In an isotropic system the mean kinetic energy $\boldsymbol{\kappa}$ of the atoms can then be calculated from

$$\boldsymbol{\kappa} = \frac{3\hbar^2}{2M}\int y^2 J(y)dy. \tag{3}$$

For a Gaussian $J(y)$

$$J(y) = \frac{1}{\sqrt{2\pi\sigma^2}}\exp\left(-\frac{y^2}{2\sigma^2}\right), \tag{4}$$

and $\boldsymbol{\kappa} = 3/2\hbar^2\sigma^2/M$. The IA is strictly valid only in the limit of infinite q. Corrections at finite q are $\sim\bar{p}/q$, where $\bar{p}$ is the mean atomic momentum [24]. The measurements described here were performed with $110\ \text{Å}^{-1} < q < 130\ \text{Å}^{-1}$. Since the measured value of $\bar{p}/\hbar \sim 1\ \text{Å}^{-1}$, corrections to the IA are ~1%—less than the statistical error. Thus these corrections were neglected in the analysis.

Three different samples were prepared to test the effects of crystal quality and ^{3}He impurity concentration, which are thought to be important for the observation of supersolidity [2,17]. In order to provide the conditions necessary for growing a good ^{4}He single crystal a cylindrical cell made of aluminum alloy 7075 with inner diameter 20 mm, internal length 55.5 mm, wall thickness 0.7 mm, and incorporating a Bridgman seal was designed to hold a working pressure up to 100 bar. The cell was attached with the cylinder axis vertical to the mixing chamber of an Oxford Instruments Kelvinox VT dilution refrigerator. The fully calibrated ruthenium-oxide temperature sensor was mounted on the mixing chamber of the refrigerator. The high purity ^{4}He gas (Air Products BIP grade ~0.3 ppm ^{3}He) was condensed into the cell through a stainless steel capillary with inner diameter 0.41 mm thermally anchored at the mixing chamber, heat-exchanger, still chamber, and 1 K pot.

In order to prepare sample A, helium was initially condensed into the cell at temperature ~2 K until the cell was completely filled. The cell temperature was increased and controlled at 2.9 K. The ^{4}He pressure was then raised slowly up to 70 bar. At that point the temperature was quickly dropped by 100 mK and the capillary was blocked by a solid helium plug. The temperature was then decreased by 100 mK each hour until 2 K where it was kept for another 8 h. The sample was then cooled to the base temperature of the dilution refrigerator. The density of the solid sample obtained from observed diffraction peaks was 31.2 atoms/nm^3 (see Table II) and at low-temperatures (less than 1 K) the sample pressure was 40.6 bar [25]. The scarcity of observable Bragg peaks is consistent with the presence of an hcp single crystal. The observation of (100) and (101) peaks but no (001) peak in the horizontal plane, implies that the crystal was oriented with c axis along the (vertical) axis of the cylinder.

In the preparation of sample B the sample was warmed to the liquid phase at 3.4 K and 70 bar and then cooled quickly to base temperature (3.4 − 1.5 K in 7.5 min, 1.5 − 0.8 K in 50 min, 0.8 K to 0.2 K in 10 min and 0.2 − 0.07 K in 50 min). To prepare sample C, the helium was removed from the cell and replaced with a ^{3}He-^{4}He mixture containing 10 ppm of ^{3}He. The sample was then cooled rapidly from 3.5 K at 70 bar (3.5 − 1.5 K in 5 min, 1.5 − 1.0 K in 50 min, 1.0 − 0.1 K in 10 min). Diffraction measurements showed many Bragg peaks in both samples B and C, implying that they were polycrystalline. Within measurement error samples B and C had the same density as sample A (see Table II).

The data was analyzed by fitting Eq. (4) convolved with the instrument resolution function. The latter was determined by fitting to liquid data collected at a temperature of 2.5 K for which $\boldsymbol{\kappa} = 15.8$ K [21,26]. The peak positions are determined by the kinematics of the scattering process via Eq. (1). Hence the fitting parameters are a Gaussian standard deviation and amplitude for each peak. In order to fit the cryostat peak accurately an essentially empirical procedure was used. Three different Gaussians were fitted to the can peak; mass 27 (corresponding to the sample cell and aluminum tails of the cryostat) and two fictitious masses of 20 and 40. The latter peaks were of small amplitude and are well separated from the He peak. They were necessary to allow for the different times of flight from cryostat tails on either side of the sample. This

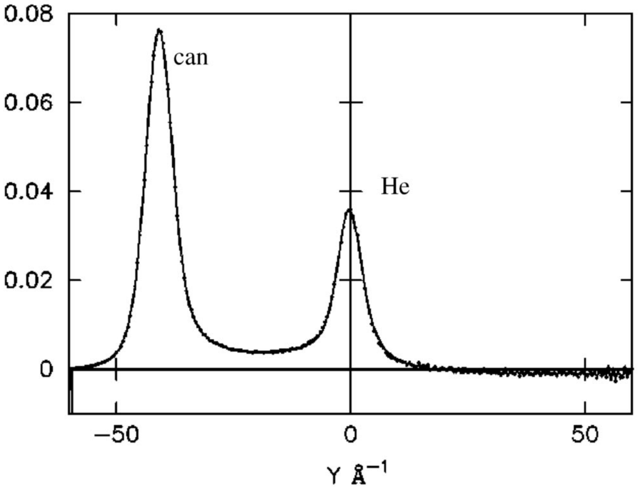

FIG. 1. Data points with error bars and fit (solid line) for sample + can after focusing 88 detectors in the ^{4}He y space. Units of the vertical axis are arbitrary.

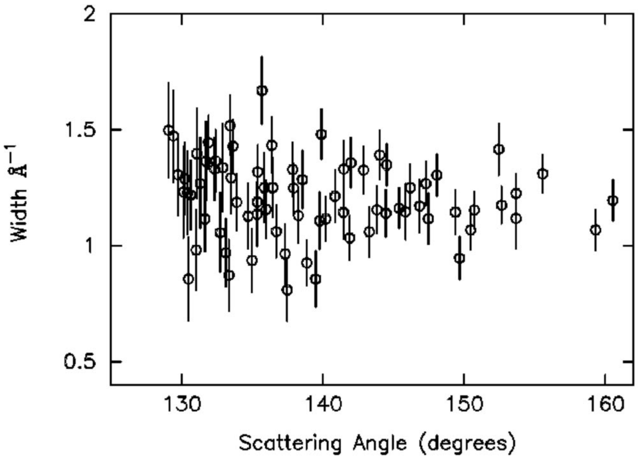

FIG. 2. Values of σ obtained from individual detectors for sample A at 0.400 K as a function of the scattering angle.

procedure was followed in preference to a direct subtraction of the can peak in order to increase the statistical accuracy of the measurements. Figure 1 illustrates the quality of the fits obtained.

In each run the Gaussian standard deviation σ of the He peak was determined for each of the 88 detectors. Figure 2 shows a typical data set with the individual σ values shown as a function of scattering angle.

A very relaxed energy resolution was employed in order to increase the statistical accuracy of the measurements. Figure 3 shows the focused data in the y space for ^{4}He as points with statistical error bars, after subtraction of the contribution from the cryostat and sample container. The solid line is the fit and the dotted line is the instrument resolution function. Despite the rather poor resolution, which rules out any detailed line shape analysis, kinetic energies can be obtained quite accurately by this procedure. A VESUVIO measurement on liquid helium [27] using the same technique showed a sharp change in the atomic kinetic energy of ~10% at the superfluid transition and quite accurately reproduced calculated and previously measured values of $\boldsymbol{\kappa}$.

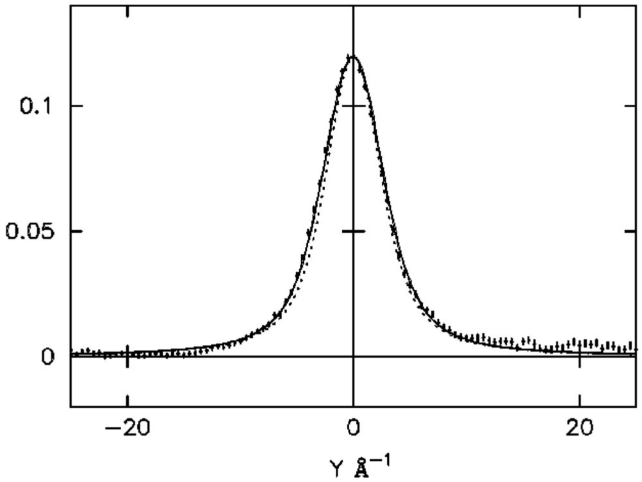

FIG. 3. Data in He y space for sample A at 0.400 K after can subtraction. The points are the data from all detectors after focusing in y space. The solid line is the fit and the dotted line is the instrument resolution function. The integrated area under the distribution has been normalized to unity.

TABLE I. Fitted widths and corresponding kinetic energies for the different samples at the measured temperatures.

Sample	T (K)	σ (Å^{-1})	K (K)
A	0.115 (4)	1.207 (14)	26.5 (6)
A	0.400 (7)	1.227 (14)	27.4 (6)
A	0.150 (4)	1.200 (13)	26.2 (6)
A	0.070 (4)	1.220 (16)	27.1 (7)
B	0.075 (4)	1.209 (14)	26.6 (6)
C	0.075 (4)	1.191 (14)	25.8 (6)

The σ values and the corresponding kinetic energies obtained in each run were obtained by performing a weighted average over the values obtained from individual detectors. The results with statistical errors are listed in Table I and the values of kinetic energy obtained are shown in Fig. 4. The values obtained are consistent with those previously measured at 1.7 K [28].

The VESUVIO detectors also allow for a relatively crude measurement of diffraction spectra. They are composed of 1 cm thickness of ^{6}Li-doped scintillator glass, to give a high neutron detection efficiency at eV energies. Although the thick glass gives peak shapes which are difficult to characterize and the high background makes the estimation of peak amplitudes difficult, changes in lattice parameter with temperature can be measured to ~0.05%. The lattice parameters were obtained from the different runs and used to calculate the sample density. The results are given in Table II.

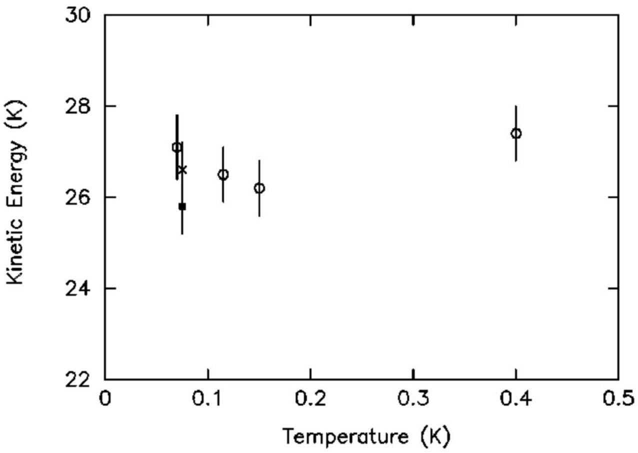

FIG. 4. Kinetic energies for different runs. The open circles are results from sample A. The cross from sample B and the solid square from sample C.

TABLE II. The three longest lattice spacings in Å observed in the different runs. Column 5 contains the calculated sample density and column 6 the corresponding molar volume.

Sample	(101)	(002)	(100)	Density (atoms/nm^3)	Molar Volume (cm^3)
A (0.115 K)	2.759 (7)		3.1055	31.2 (3)	19.3 (2)
A (0.400 K)	2.759 (7)		3.1055	31.2 (3)	19.3 (2)
A (0.150 K)	2.758 (7)		3.1056	31.2 (3)	19.3 (2)
A (0.070 K)	2.758 (7)		3.1055	31.2 (3)	19.3 (2)
B (0.075 K)	2.758 (2)	2.934 (4)	3.131 (2)	30.6 (3)	19.7 (2)
C (0.075 K)	2.757 (3)	2.940 (3)	3.128 (2)	30.6 (3)	19.7 (2)

The errors on the lattice spacings were the standard deviations of the determinations from the Bragg peaks observed in different detectors. For sample A the (101) peak was observable only in 2 detectors, the (100) peak in a single detector and (002) was not observed at all. The absolute value of the *d* spacing of the (100) peak in sample A is uncertain to ~1%, due to the finite width of the detectors. To within 1 part in 2000 no change in the lattice parameters was observed as the temperature was changed in sample A.

The data presented here should be compared with analogous data on superfluid liquid ^{4}He. In the latter case experiment [20,21] and calculation [26] show that the kinetic energy decreases by 11%–12% as the temperature is lowered through the superfluid transition. This is associated with the development of a 7%–8% Bose condensate fraction with zero kinetic energy. Neutron [29,30] and x-ray [31] diffraction also reveal a significant change in structure as the liquid is cooled through the superfluid transition. The liquid becomes more disordered, consistent [32] with the development of ~10% more spaces in the liquid structure. In contrast the measurements presented here imply that the vacancy concentration in the solid does not change to within ~0.1% as it is cooled through the supersolid transition region. Our results suggest that the supersolid transition in ^{4}He has a different microscopic origin to the superfluid transition in the liquid.

We gratefully acknowledge help from the ISIS sample environment group; in particular, A. Church and C. Goodway for the pressure rig, J. Keeping for dilution refrigerator support, R. Done and M. Chowdhury for design and manufacture of the pressure cell.

[1] E. Kim and M. H. W. Chan, Nature (London) **427**, 225 (2004).
[2] E. Kim and M. H. W. Chan, Science **305**, 1941 (2004).
[3] E. Kim and H. W. Chan, Phys. Rev. Lett. **97**, 115302 (2006).
[4] A. S. Rittner and J. D. Reppy, cond-mat/0604528.
[5] M. Kubota *et al.* (to be published).
[6] K. Shirahama *et al.*, http://online.kitp.ucsb.edu/online/smatter_m06/shirahama/.
[7] A. F. Andreev and I. M. Lifshitz, Sov. Phys. JETP **29**, 1107 (1969).
[8] G. V. Chester, Phys. Rev. A **2**, 256 (1970).
[9] A. J. Leggett, Phys. Rev. Lett. **25**, 1543 (1970).
[10] B. K. Clark and D. M. Ceperley, Phys. Rev. Lett. **96**, 105302 (2006).
[11] A. C. Clark and M. H. W. Chan, J. Low Temp. Phys. **138**, 853 (2005).
[12] X. Dai, M. Ma, and F.-C. Zhang, Phys. Rev. B **72**, 132504 (2005).
[13] P. W. Anderson, W. F. Brinkman, and D. A. Huse, Science **310**, 1164 (2005).
[14] M. Boninsegni *et al.*, Phys. Rev. Lett. **97**, 080401 (2006).
[15] D. E. Galli and L. Reatto, Phys. Rev. Lett. **96**, 165301 (2006).
[16] I. A. Todoshenko *et al.*, cond-mat/0607081.
[17] S. Sasaki *et al.*, Science **313**, 1098 (2006).
[18] J. Day, T. Herman, and J. Beamish, Phys. Rev. Lett. **95**, 035301 (2005).
[19] J. Day and J. Beamish, Phys. Rev. Lett. **96**, 105304 (2006).
[20] T. R. Sosnick, W. M. Snow, and P. E. Sokol, Europhys. Lett. **9**, 707 (1990).
[21] R. T. Azuah, W. G. Stirling, H. R. Glyde, M. Boninsegni, P. E. Sokol, and S. M. Bennington, Phys. Rev. B **56**, 14 620 (1997).
[22] J. Maynard, Phys. Rev. B **14**, 3868 (1976).
[23] J. Mayers and T. Abdul-Redah, J. Phys. Condens. Matter **16**, 4811 (2004).
[24] See H. R. Glyde, Phys. Rev. B **50**, 6726 (1994) for a recent review of the literature on final state effects.
[25] A. Driessen, E. van der Poll, and I. F. Silvera, Phys. Rev. B **33**, 3269 (1986).
[26] D. M. Ceperley and E. L. Pollock, Phys. Rev. Lett. **56**, 351 (1986).
[27] J. Mayers, F. Albergamo, and D. Timms, Physica (Amsterdam) **B276**, 811 (2000).
[28] D. M. Ceperley *et al.*, Phys. Rev. Lett. **77**, 115 (1996).
[29] V. F. Sears and E. C. Svensson, Phys. Rev. Lett. **43**, 2009 (1979).
[30] E. C. Svensson, V. F. Sears, A. D. B. Woods, and P. Martel, Phys. Rev. B **21**, 3638 (1980).
[31] H. N. Robkoff, D. A. Ewen, and R. B. Hallock, Phys. Rev. Lett. **43**, 2006 (1979).
[32] J. Mayers, Phys. Rev. Lett. **84**, 314 (2000).